

Stereoisomeric 2-butylphenylsulfoxides and their binding modes in the adduct formation with an enantiopure dirhodium tetracarboxylate complex

Jens T. Mattiza, Vera J. Meyer, Helmut Duddeck*

Institute of Organic Chemistry, Leibniz University Hannover, Schneiderberg 1B, D-30167 Hannover, Germany

ARTICLE INFO

Article history:

Received 16 November 2009

Received in revised form 21 January 2010

Accepted 21 January 2010

Available online 1 February 2010

This paper is dedicated to Prof. Dr. Heinz Oberhammer, Eberhard Karls Universität Tübingen, Tübingen, Germany, on the occasion of his 70th birthday.

Keywords:

Chiral sulfoxides

Dirhodium complex

Conformational analysis

¹H and ¹³C NMR

Adduct formation

Chiral differentiation

ABSTRACT

All stereoisomers of the 2-butylphenylsulfoxides **1a** and **2a** and their *p*-substituted derivatives **1b–1e** and **2a–2e** (X = F, Br, NO₂, and OCH₃) were synthesized. Absolute configurations were derived from commercial enantiopure 2-butanols used as starting materials, by X-ray diffraction and by polarimetry. Preferred conformations were determined by density functional and second-order Møller–Plesset calculations. Oxygen atoms dominate in the adduct formation equilibria of 2-butylsubstituted sulfoxides and the chiral dirhodium complex **Rh*** although the sulfur atom is, in principle, the stronger donor. This is due to steric shielding of the sulfur atom produced by the aromatic ring and the secondary 2-butyl substituent. Enantiodifferentiation of sulfoxides is easily accomplished by the dirhodium experiment, i.e. recording NMR spectra in the presence of an equimolar amount of **Rh***. Complex formation shifts ($\Delta\delta$) and diastereomeric dispersion effects ($\Delta\nu$) differ in the dirhodium experiment for nonracemic mixtures of sulfoxides as compared to pure enantiomers. This, however, does not affect the efficiency of the dirhodium experiment at all.

© 2010 Elsevier B.V. All rights reserved.

1. Introduction

Dirhodium complexes and their adducts have been the focus of interest for many years [1]. They were introduced as homogeneous catalysts in various reactions [2] and found even medicinal application [3]. During the last decade, we have shown that the enantiomers of many chiral ligands, particularly those of soft Lewis bases, can be differentiated easily by adding an equimolar amount of the dirhodium complex Rh₂^(II) [(R)-(+)-MTPA]₄ (**Rh***, MTPA-H = methoxytrifluoromethylphenylacetic acid ≡ Mosher's acid; see Scheme 1) [4] to their CDCl₃ solution and monitoring the diastereomeric dispersion $\Delta\nu$ of their ¹H or ¹³C NMR signals at room-temperature (dirhodium method) [5–7].

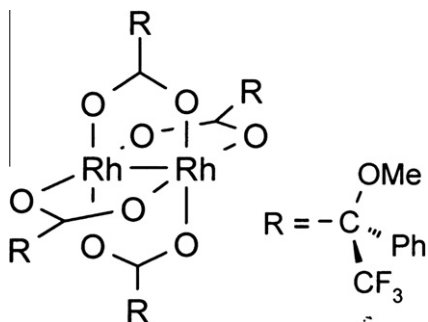
The complexation site of ligand molecules **L** in dirhodium complex adducts (**Rh*** ← **L**) can be identified by moderate deshieldings of nearby ¹H and – particularly – ¹³C nuclei (complexation shifts $\Delta\delta$). In a qualitative interpretation of positive $\Delta\delta$ values, one can assume that an adduct formation induces an increase of the electron-acceptor properties of the binding atom [5]. Recently, we investigated some ethers **3** (Scheme 2) with oxygen binding sites attached to aromatic and aliphatic ring systems [8]. In ethers, the binding en-

ergy is based primarily on electrostatic interaction [9]. As expected, we found that the inductive effect of the oxygen on the aliphatic α -carbons is enhanced when it is complexed to the rho atom ($\Delta\delta > 0$). However, deshielding complexation shifts $\Delta\delta$ at the aromatic *ipso*-carbons (also α -positioned) turned out to be minute whereas *ortho*- and *para*-carbon signals are influenced significantly by the resonance effect of oxygen and its interaction with substituents in *para*-position [8].

In order to gain further insight into the complexation mechanisms of chalcogen ligands, we extended this study to structurally analogous thioethers **4** (Scheme 2) [10]. Whereas ethers are hard ligands, thioethers are soft [11] and represent a different ligand category in the dirhodium experiment as compared to ethers [5]; i.e., thioethers can make use of an additional orbital interaction (HOMO–LUMO) for complexation. Indeed, this can be monitored by inspecting the dependence of complexation shifts at the aliphatic α carbon (C-2) and the *ortho*-carbon (C-2') on Hammett's inductive and resonance parameters, respectively [10]. For each carbon site and each parameter the correlations are opposite as compared to those of ethers, and this can be rationalized semi-quantitatively by effects of HOMO–LUMO energy changes on ¹³C chemical shifts [10].

Then, we extended these studies to sulfoxides offering both types of donors simultaneously, soft sulfur and hard oxygen atoms; the results are presented here.

* Corresponding author. Tel.: +49 511 762 4615; fax: +49 511 762 4616.
E-mail address: duddeck@mbox.oci.uni-hannover.de (H. Duddeck).



Scheme 1. Structure of the dirhodium complex Rh^* .

2. Experiment

2.1. Materials and synthesis

The syntheses of Rh^* [4], the ethers **3** [8] and the thioethers **4** [10] have been described by us earlier. The sulfoxides **1a–1e** and **2a–2e** were prepared by H_2O_2 oxidation of the thioethers **4a–4e**, respectively [12]. General procedure: the respective 2-butylphenylthioether (2.2 mmol) was dissolved in 5 ml methanol. A solution of H_2SO_4 (16%) in *tert*-butanol and 35% H_2O_2 (0.18 g, 5.1 mmol) was added dropwise. Then, the mixture was stirred for 24 h at room-temperature. Aqueous NaCl solution (5%) was added

and the mixture extracted three times with 5 ml chloroform each. The combined organic phases were dried over $MgSO_4$ and the solvent evaporated *in vacuo*. The residue was purified by column chromatography at normal pressure and temperature using silica gel as stationary and mixtures of petrol ether and ethyl acetate as mobile phase (see Section 2). Yields are given below. Synthetic procedures were not optimized. *p*-Nitrophenyl-methylsulfoxide (**5**) was prepared analogously from the respective commercially available thioether [13].

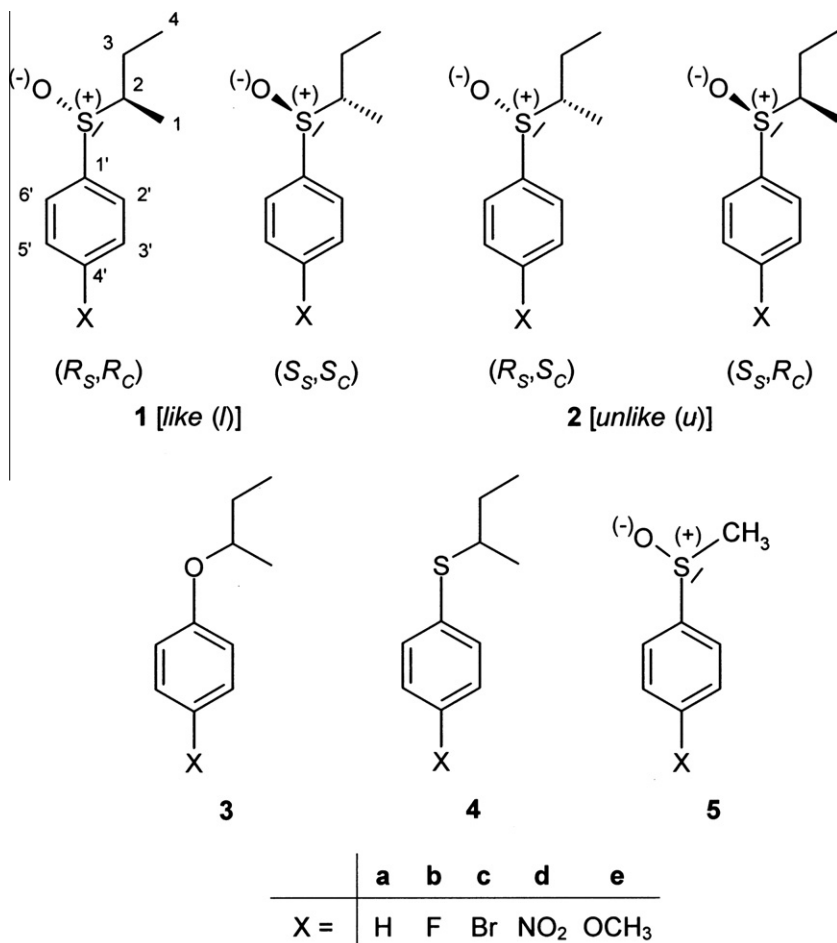
The parent sulfoxides **1a/2a** has been described in literature [14]; all others are new. We collected the 1H and ^{13}C NMR data of all enantiopure 2-butylphenylsulfoxides in Table 2; yields, physical data, infra-red (IR) and mass spectral data (ESI-MS) are listed below. IR spectra were recorded on a Bruker Vector 22 using neat samples and positive ESI-MS spectra on a Micromass LCT.

2.1.1. (R_S,R_C)- or (S_S,S_C)-(1-methylpropylthio)benzene-*S*-oxide (**1a**)

Yield: 72%, viscous, slightly yellowish liquid. IR (liquid) $\tilde{\nu}$ (cm^{-1}) 3046, 2966, 2932, 1583, 1443, 1381, 1035, 748, 692. ESI-MS calculated for $C_{10}H_{15}OS$: 183.0844 $[M+H]^+$, found: 183.0840.

2.1.2. (R_S,S_C)- or (S_S,R_C)-(1-methylpropylthio)benzene-*S*-oxide (**2a**)

Yield: 73%, viscous, slightly yellowish liquid. IR (liquid) $\tilde{\nu}$ (cm^{-1}) 3040, 2963, 2932, 1581, 1441, 1384, 1031, 748, 691. ESI-MS calculated for $C_{10}H_{15}OS$: 183.0844 $[M+H]^+$, found: 183.0843.



Scheme 2. Structures of stereoisomeric 2-butylphenylsulfoxides **1** (*like*) and **2** (*unlike*); structurally related ethers **3** and thioethers **4** for comparison. Although the atom numbering is not in total agreement with the IUPAC nomenclature, it has been chosen to for a better comparability of NMR data. Correct IUPAC names are given in the Experimental Part.

Table 1
Crystallographic data and structure refinement for (*R_SS_C*)-**2d** (*ul*) and selected bond lengths (in pm), bond angles (in °) and torsion angles (in °).^a

	(<i>R_SS_C</i>)- 2d	Selected parameters	
Chemical formula	C ₁₀ H ₁₃ NO ₃ S	S–O	1.496(3)
Formula weight	227.27 g/mol	S–C2	1.798(5)
Temperature	297 K	S–C1'	1.779(4)
Crystal system, space group	Orthorhombic, <i>P</i> 2 ₁ 2 ₁ 2 ₁	O–S–C2	107.7(2)
Unit cell parameters		O–S–C1'	106.4(7)
<i>a</i> = 9.049(3)	$\alpha = \beta = \gamma = 90^\circ$	C1–C2–S	113.5(4)
<i>b</i> = 10.448(4)		C3–C2–S	107.1(4)
<i>c</i> = 12.547(8)		C2'–C1'–S	119.8(3)
Cell volume	1186.2(10)	C6'–C1'–S	120.9(3)
<i>Z</i>	4	O–S–C2–C1	–51.94
Calculated density	1.273 g/cm ³	O–S–C2–C3	+71.56
Absorption coefficient	0.260 mm ^{–1}	O–S–C1'–C2'	–9.68
Crystal color and size	White, 0.31 × 0.29 × 0.11 mm	C2–S–C1'–C2'	–121.11
Reflections collected	16,664	C3–C2–S–C1'	–178.53
Independent reflections	2329	O–N–C4'–C3'	+167.80
Reflections with <i>I</i> > 2σ(<i>I</i>)	1358		
Minimum and maximum transmission	$\theta_{\min} = 2.5^\circ$, $\theta_{\max} = 26.1^\circ$		
Final <i>R</i> indices [<i>I</i> > 2σ(<i>I</i>)]	<i>R</i> ₁ = 0.0501, <i>wR</i> ₂ = 0.1125		
<i>R</i> indices (all data)	<i>R</i> ₁ = 0.0879, <i>wR</i> ₂ = 0.1280		
Goodness-of-fit on <i>F</i> ²	1.005		
Largest difference map peak and hole	0.372 eÅ ^{–3} , –0.202 eÅ ^{–3}		
Flack parameter	–0.01(19)		

^a The geometric parameters of the enantiomeric (*S_SR_C*)-**2d** are the same within the experimental error limits; of course, torsion angles have opposite signs.

Table 2
¹H and ¹³C chemical shifts (δ) of the sulfoxides **1** and **2** (Scheme 2); in ppm, solvent: CDCl₃, relative to internal tetramethylsilane δ = 0 ppm.^{a,b}

	1a/2a X = H (<i>l</i>)/(<i>u</i>)	1b/2b^c X = F (<i>l</i>)/(<i>u</i>)	1c/2c X = Br (<i>l</i>)/(<i>u</i>)	1d/2d X = NO ₂ (<i>l</i>)/(<i>u</i>)	1e/2e X = OCH ₃ (<i>l</i>)/(<i>u</i>)
H-1	1.09/1.06	1.07/1.05	1.11/1.06	1.19/1.03	1.06/1.03
H-2	2.72/2.55	2.70/2.52	2.71/2.51	2.78/2.60	2.70/2.67
H-3 ^d	<i>a</i> : 1.46/1.48 <i>b</i> : 1.81/1.94	<i>a</i> : 1.45/1.45 <i>b</i> : 1.80/1.92	<i>a</i> : 1.45/1.46 <i>b</i> : 1.77/1.94	<i>a</i> : 1.48/1.57 <i>b</i> : 1.72/2.01	<i>a</i> : 1.43/1.45 <i>b</i> : 1.86/1.84
H-4	1.01/1.09	1.02/1.09	1.01/1.11	1.04/1.15	1.04/1.05
H-2'/H-6'	7.62/7.57	7.62/7.56	7.49/7.44	7.80/7.76	7.54/7.55
H-3'/H-5'	7.51/7.50	7.22/7.21	7.66/7.65	8.38/8.38	7.01/7.02
H-4'	7.51/7.52	–	–	–	–
OCH ₃	–	–	–	–	3.86/3.86
C-1	11.8/10.2	11.7/10.1	11.8/10.1	12.1/10.0	11.6/10.5
C-2	61.0/61.1	61.1/61.2	61.1/61.3	61.4/61.7	61.0/61.1
C-3	22.0/23.8	22.1/23.5	22.0/23.8	21.7/24.2	22.3/23.3
C-4	10.9/11.6	10.9/11.5	11.0/11.6	11.0/11.7	10.9/11.5
C-1'	141.5/141.7	136.9/137.4	140.6/141.3	149.3/149.3	132.3/132.8
C-2'/C-6'	125.3/124.7	127.6/126.8	126.9/126.3	126.3/125.7	127.2/126.5
C-3'/C-5'	128.8/128.9	116.2/116.2	132.1/132.1	123.9/124.0	114.4/114.4
C-4'	131.0/130.7	164.4/164.1	125.6/125.1	149.6/150.2	162.0/161.7
OCH ₃	–	–	–	–	55.4/55.5

^a Values left of the slash: like-isomer (*l*) (*R_SR_C*)-**1** or (*S_SS_R*)-**1**; values right of the slash: unlike-isomer (*u*) (*R_SS_C*)-**2** or (*S_SR_C*)-**2**.

^b ¹H, ¹H coupling constants in the 2-butyl residue are uniform for diastereomers regardless of the substituent X: **1a–1e** (like), ²J(H-3a,H-3b) = 13.9 ± 0.1 Hz, ³J(H-1,H-2) = 6.9 ± 0.1 Hz, ³J(H-2,H-3a) = 9.1 ± 0.1 Hz, ³J(H-2,H-3b) = 4.1 ± 0.1 Hz, ²J(H-3a,H-4) = ³J(H-3b,H-4) = 7.5 ± 0.1 Hz; **2a–2e** (unlike), ²J(H-3a,H-3b) = 14.1 ± 0.1 Hz, ³J(H-1,H-2) = 6.9 ± 0.1 Hz, ³J(H-2,H-3a) = 6.9–8.1 Hz, ³J(H-2,H-3b) = 5.8–6.6 Hz, ³J(H-3a,H-4) = ³J(H-3b,H-4) = 7.5 ± 0.1 Hz.

^c Coupling constants involving ¹⁹F: **1b**, ³J(¹⁹F,¹H) = 8.8 Hz (H-3'/5'), ⁴J(¹⁹F,¹H) = 8.5 Hz (H-2'/6'), ¹J(¹⁹F,¹³C) = 245.6 Hz (C-4'), ²J(¹⁹F,¹³C) = 21.2 Hz (C-3'/5'), ³J(¹⁹F,¹³C) = 8.3 Hz (C-2'/6'), ⁴J(¹⁹F,¹³C) = 3.1 Hz (C-1'), ⁶J(¹⁹F,¹³C) = 1.0 Hz (C-2); **2b**, ³J(¹⁹F,¹H) = 9.0 Hz (H-3'/5'), ⁴J(¹⁹F,¹H) = 8.8 Hz (H-2'/6'), ¹J(¹⁹F,¹³C) = 243.1 Hz (C-4'), ²J(¹⁹F,¹³C) = 21.6 Hz (C-3'/5'), ³J(¹⁹F,¹³C) = 8.0 Hz (C-2'/6'), ⁴J(¹⁹F,¹³C) = 2.9 Hz (C-1').

^d Diastereotopic atoms H-3a and H-3b with δ(H-3a) < δ(H-3b) in all derivatives; for the stereochemical assignment see text.

2.1.3. (*R_SR_C*)- or (*S_SS_C*)-4-fluoro-1(1-methylpropylthio)benzene-S-oxide (**1b**)

Yield, 51%, m.p. 71–72 °C. IR (solid) $\tilde{\nu}$ (cm^{–1}) 3050, 2968, 2933, 1589, 1491, 1460, 1382, 1220, 834. ESI-MS calculated for C₁₀H₁₄FOS: 201.0749 [M+H]⁺, found: 201.0747.

2.1.4. (*R_SS_C*)- or (*S_SR_C*)-4-fluoro-1(1-methylpropylthio)benzene-S-oxide (**2b**)

Yield, 47%, m.p. 70–71 °C. IR (solid) $\tilde{\nu}$ (cm^{–1}) 3046, 2966, 2937, 1592, 1487, 1460, 1380, 834. ESI-MS calculated for C₁₀H₁₄FOS: 201.0749 [M+H]⁺, found: 201.0756.

2.1.5. (*R_SR_C*)- or (*S_SS_C*)-1-bromo-4(1-methylpropylthio)benzene-S-oxide (**1c**)

Yield: 62%, viscous, slightly yellowish liquid. IR (liquid) $\tilde{\nu}$ (cm^{–1}) 3042, 2966, 2931, 1571, 1471, 1385, 1063, 1036, 817. ESI-MS calculated for C₁₀H₁₄BrOS: 260.9949 [M+H]⁺, found: 260.9954.

2.1.6. (*R_SS_C*)- or (*S_SR_C*)-1-bromo-4(1-methylpropylthio)benzene-S-oxide (**2c**)

Yield: 62%, viscous, slightly yellowish liquid. IR (liquid) $\tilde{\nu}$ (cm^{–1}) 3038, 2966, 2924, 1570, 1461, 1385, 1061, 1036, 814. ESI-MS calculated for C₁₀H₁₄BrOS: 260.9949 [M+H]⁺, found: 260.9953.

2.1.7. (R_S,R_C)- or (S_S,S_C)-4-nitro-1(1-methylpropylthio)benzene-S-oxide (**1d**)

Yield: 74%, m.p. 82–83 °C. IR (solid) $\tilde{\nu}$ (cm^{-1}) 3050, 2968, 2932, 1602, 1521, 1343, 1038, 852. ESI-MS calculated for $\text{C}_{10}\text{H}_{14}\text{NO}_3\text{S}$: 228.0694 $[\text{M}+\text{H}]^+$, found: 228.0689.

2.1.8. (R_S,S_C)- or (S_S,R_C)-4-nitro-1(1-methylpropylthio)benzene-S-oxide (**2d**)

Yield: 76%, m.p. 79–81 °C. IR (solid) $\tilde{\nu}$ (cm^{-1}) 3050, 2968, 2928, 1600, 1523, 1343, 1037, 850. ESI-MS calculated for $\text{C}_{10}\text{H}_{14}\text{NO}_3\text{S}$: 228.0694 $[\text{M}+\text{H}]^+$, found: 228.0698.

2.1.9. (R_S,R_C)- or (S_S,S_C)-4-methoxy-1(1-methylpropylthio)benzene-S-oxide (**1e**)

Yield: 94%, viscous, slightly yellowish liquid. IR (liquid) $\tilde{\nu}$ (cm^{-1}) 3042, 2968, 1602, 1583, 1459, 1038, 850. ESI-MS calculated for $\text{C}_{10}\text{H}_{14}\text{NO}_3\text{S}$: 213.0949 $[\text{M}+\text{H}]^+$, found: 213.0947.

2.1.10. (R_S,S_C)- or (S_S,R_C)-4-methoxy-1(1-methylpropylthio)benzene-S-oxide (**2e**)

Yield: 96%, viscous, slightly yellowish liquid. IR (liquid) $\tilde{\nu}$ (cm^{-1}) 3051, 2970, 1606, 1582, 1449, 1040, 850. ESI-MS calculated for $\text{C}_{10}\text{H}_{14}\text{NO}_3\text{S}$: 213.0949 $[\text{M}+\text{H}]^+$, found: 213.0952.

2.1.11. rac-4-Nitro-1-methylthiobenzene-S-oxide (**5**)

Yield: 24%, yellowish solid, m.p. 147–149 °C. IR (solid) $\tilde{\nu}$ (cm^{-1}) 3099, 3022, 2390, 1514, 1474, 1338, 1306, 1086, 1044, 850, 740. ESI-MS calculated for $\text{C}_7\text{H}_7\text{NO}_3\text{S}$: 186.0225 $[\text{M}+\text{H}]^+$, found: 186.0223.

NMR, in CDCl_3 , δ (ppm): 2.80 (H-1, methyl); 7.84 (H-2'/6'); 8.40 (H-3'/5'); 43.9 (C-1, methyl); 149.5 (C-1', ipso); 124.7 (C-2'/6', ortho); 124.5 (C-3'/5', meta); 153.2 (C-4', para); $\Delta\delta$ (ppm)/ $\Delta\nu$ (Hz) + 1 eq. Rh^* : +0.62/4 (H-1, methyl); +0.21/not detectable (H-2'/6'); –0.30/not detectable (H-3'/5'); –3.2/51 (C-1, methyl); –1.5/11 (C-1', ipso); +1.4/6 (C-2'/6', ortho); –0.5/5 (C-3'/5', meta); –3.8/6 (C-4', para); $\Delta\delta$ (ppm)/ $\Delta\nu$ (Hz) + 2 eq. Rh^* : +0.82/9 (H-1, methyl); +0.28/9 (H-2'/6'); –0.45/35 (H-3'/5'); –4.7/62 (C-1, methyl); –3.3/11 (C-1', ipso); +1.7/3 (C-2'/6', ortho); –0.3/12 (C-3'/5', meta); –3.9/12 (C-4', para).

2.2. Liquid chromatography

Column chromatography was performed at atmospheric pressure using silica gel 60 M, 230–400 mesh (Merck) as stationary and a mixture of petrol ether and ethyl acetate (1:1) as mobile phase.

2.3. NMR spectroscopy

All NMR measurements were performed in analogy to those described for the corresponding ethers **3** [8]; details of the one- and two-dimensional NMR experiments (DEPT 90 and DEPT 135, gradient-selected COSY, HMQC and HMBC spectra) can be found in this reference.

^1H (400.1 MHz) and ^{13}C (100.6 MHz) NMR measurements were recorded at room-temperature on a Bruker Avance DPX-400 spectrometer. Samples were ca 0.01–0.025 mmol in CDCl_3 . The chemical shift reference was internal tetramethylsilane ($\delta = 0$ ppm).

In the standard dirhodium experiment, Rh^* and equimolar amounts of the ligands **1a–1e**, **2a–2e** and **5** (Scheme 2), respectively, were dissolved in 0.7 ml CDCl_3 ; quantities of 10–25 mg of Rh^* (ca. 0.01–0.025 mmol concentration) were employed. If necessary, the dissolution process can be accelerated by exposing NMR sample tubes to an ultrasonic bath for a few minutes. In earlier reports on soft-base ligands, the use of acetone- d_6 for increasing the solubility of Rh^* had been recommended [5]. This auxiliary, how-

ever, should be avoided when hard-base ligands like oxygen functionalities are involved because acetone- d_6 is a serious competitor in the adduct formation in such cases.

Note that $\Delta\nu$ values are B_0 -dependent. They are quoted with signs because nonracemic mixtures with known enantiomeric composition have been used; the definitions are: $\Delta\nu = \nu(R_S R_C) - \nu(S_S S_C)$ for like-sulfoxides **1** and $\Delta\nu = \nu(R_S S_C) - \nu(S_S R_C)$ for unlike-sulfoxides **2**. All dispersion values are given as integers in Hz as determined at $B_0 = 9.4$ Tesla corresponding to 400 MHz ^1H and 100.6 MHz ^{13}C .

2.4. Polarimetry

Using a Perkin–Elmer Polarimeter 341, specific rotations (at 589 nm) of the enantiomers with (R_C)-configuration were measured in methanol at room-temperature; concentrations (in g/ml) are given in parentheses; $[\alpha]_D$: **1a**, +106.8 (0.0082); **1b**, +82.3 (0.0074); **1c**, +91.6 (0.0154); **1d**, +73.1 (0.0036); **1e**, +146.2 (0.0099); **2a**, –215.0 (0.0120); **2b**, –188.2 (0.0079); **2c**, –165.8 (0.0147); **2d**, –167.1 (0.0084); **2e**, –168.7 (0.0120).

2.5. Crystallography

X-ray diffraction experiments were performed using a Stoe IPDS single crystal diffractometer. Crystallographic data, the table of atomic coordinates and thermal parameters, and the full list of bond lengths and angles of (S_S,R_C)-**2d** have been deposited with the Cambridge Crystallographic Data Centre, CCDC 746478; email: deposit@ccdc.cam.ac.uk; see also Table 1. The enantiomer (R_S,S_C)-**2d** has also been examined. All data are the same except signs of torsion angles which have opposite signs.

2.6. Powder diffraction

Powder diffraction measurements were performed on a Stoe powder diffractometry system Stadi P with PSD Cu K α irradiation, anode current 30 mA, 40 kV anode voltage, range 5–100° 2θ .

2.7. Theoretical calculations

All molecular structures were calculated by density functional methods (B3LYP 6-31G* and 6-311++G**) and second-order Møller–Plesset (MP2 6-31G*) using the SPARTAN '08 program package, version 1.0.0 [15].

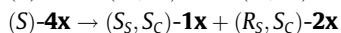
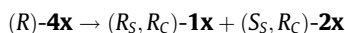
3. Results and discussion

Sulfoxides offer both types of ligand categories simultaneously, a soft sulfur atom with a free electron pair and a hard oxygen atom; the $\text{S}^{(+)}\text{--O}^{(-)}$ bond is predominantly a single bond [16]. The question is which of these two atoms, O or S, is the binding site. Moreover, sulfoxides possess a configurationally stable chirality centre at the sulfur atom, (R_S) or (S_S). If they are substituted by a chiral hydrocarbon side chain, such as (R)- and (S)-2-butyl, two diastereomeric pairs of enantiomers exist which, in the presence of the enantiopure Rh^* , are all diastereomeric and display different NMR spectral parameters. We report here our results on such molecular systems **1** and **2** (Scheme 2).

3.1. Syntheses, isolation and characterization of the four stereoisomers of 2-butylphenylsulfoxide **1a** and **2a** as well as their p -substituted derivatives (**1b–1e** and **2b–2e**)

In order to synthesize all enantiomerically pure isomers of **1a–1e** and **2a–2e**, we started from the two commercially available

enantiopure 2-butanols and prepared the respective 2-butylphenyl and their *para*-substituted derivatives **4a–4e** [10]. Oxidation [12] of those thioethers resulted in mixtures of two diastereomeric, enantiopure sulfoxides in each case ($x = a, b, c, d,$ and e ; Scheme 2):



The two diastereomers in these mixtures were isolated by liquid chromatography (for details see Section 2). In the case of the nitro derivatives **1d** and **2d**, the less polar isomer was eluted first from each of the reaction mixtures and recrystallized for X-ray diffraction experiments (Fig. 1 and Table 1; see also Section 3.2).

It turned out from those measurements that, in both cases, the less polar isomer was the *unlike*-configured, (S_S, R_C)-**2d** and (R_S, S_C)-**2d** (Fig. 1), respectively [17]; i.e., those compounds were enantiomers. Thus, the other one in each of the mixtures obtained from the oxidation reaction was the *like*-stereoisomer, (R_S, R_C)-**1d** and (S_S, S_C)-**1d**, respectively, again enantiomers. Thereby, the absolute configurations of all four stereoisomers of 2-butyl-*para*-nitro-

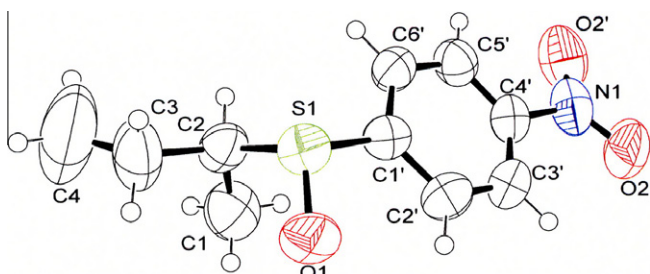


Fig. 1. ORTEP plot from the X-ray diffraction measurement of 4-nitro-1-(1-methylpropylthio)benzene-S-oxide [(R_S, S_C)-**2d**]; for discussion see text.

Table 3

Molecular geometry parameters of **2d**-conformer **B** (see Fig. 2) as calculated by density functional BYLYP and Møller–Plesset MP2 methods [15] compared with data from an X-ray diffraction measurement.

Geometry Parameters	Density functional B3LYP		MP2 6-31G*	X-ray
	6-31G*	6-311++G**		
$d(S-O)$ [pm]	151.6	151.6	151.7	149.6
$d(S-C-2)$ [pm]	188.3	188.8	184.2	177.9
$d(S-C-1')$ [pm]	182.7	183.1	180.6	179.8
$\alpha(O-S-C-2)$ [°]	107.2	107.3	106.8	106.4
$\alpha(O-S-C-1')$ [°]	106.6	106.1	106.7	107.7
$\phi(O-S-C-2-C-1)$ [°]	-45.3	-45.3	-46.5	-51.9
$\phi(O-S-C-2-C-3)$ [°]	-78.7	-79.5	-76.9	-71.6
$\phi(O-S-C-1'-C-2)$ [°]	-177.6	-178.1	-177.5	-175.3

phenylsulfoxide (**1d** and **2d**) were isolated and characterized unequivocally.

Inspecting the 1H and ^{13}C NMR chemical shift data of **1d** and **2d** (Table 2), it is evident that they differ significantly in their δ values for H-1 (1.19 vs. 1.03 ppm), H-2 (2.78 vs. 2.60 ppm), H-3 (1.48/1.72 vs. 1.57/2.01 ppm), H-4 (1.01 vs. 1.15 ppm), C-1 (12.1 vs. 10.0 ppm), and C-3 (21.7 vs. 24.2 ppm). Interestingly, analogous chemical shift differences are observed for all other derivatives, too. The reason for this systematic chemical shift divergence is, of course, the stereochemistry of the sulfoxides. Some ^{13}C and 1H chemical shift trends exerted by $S^{(+)}-O^{(-)}$ groups on neighbouring hydrogen and carbon atoms have been reported [16,18] but they were derived from compounds containing rigid six-membered rings in chair-conformation whereas the sulfoxides **1** and **2** are mixtures of more than one open-chain conformers (see below). Therefore, empirical correlations between those molecular systems with respect to effects on chemical shifts failed or appeared to be speculative.

The specific rotations $[\alpha]_D$ provided an independent tool for the differentiation of diastereomers. For the (R_C)-isomers, they are positive for the *like*- but negative for the *unlike*-diastereomers (see Section 2); vice versa for the (S_C)-isomers.

As a result, the stereochemistry of all sulfoxides could be assigned in analogy to **1d** and **2d** with a very high level of reliability.

3.2. Conformational analysis of the sulfoxides **1d** and **2d**

Theoretical density functional (B3LYP/6-21G* and 6-311++G**) as well as second-order Møller–Plesset (MP2/6-31++G**) calculations have been performed for the sulfoxides **1a/2a** ($X = H$), **1b/2b** ($X = F$) and **1d/2d** ($X = NO_2$) as isolated molecules without solvent shell. Overall, very similar energy differences for the most stable conformers resulted from these calculations regardless of the substituents so that we restrict the following discussion to the nitro derivatives **1d** and **2d** (Table 3 as well as Figs. 2 and 3, respectively) in order to compare the calculated structures with the X-ray diffraction geometries (Table 4 and Fig. 1). It should be noted that one has to accept energy error limits of 1–2 kJ/mol in such calculations so that a quantitative evaluation of the balances in the equilibria of the most stable conformers is doubtful. In the following interpretation, we excluded conformers with energies higher than 4 kJ/mol relative to that with the lowest energy.

A comparison of the calculated geometry parameters with those of the X-ray structure shows that the MP2 calculations reproduce the experimental values better than any of the density functional calculations (Table 3). This, however, does not necessarily mean that MP2-calculated energies are more reliable. Anyway, the most stable conformers which play the major role in the equilibria were reproduced satisfactorily by all calculation methods (Table 4).

We start the discussion with the *unlike*-isomer **2d** because we have an X-ray structure of that diastereomer: Fig. 2 shows the two calculated conformers of (R_S, S_C)-**2d** with the lowest calculated

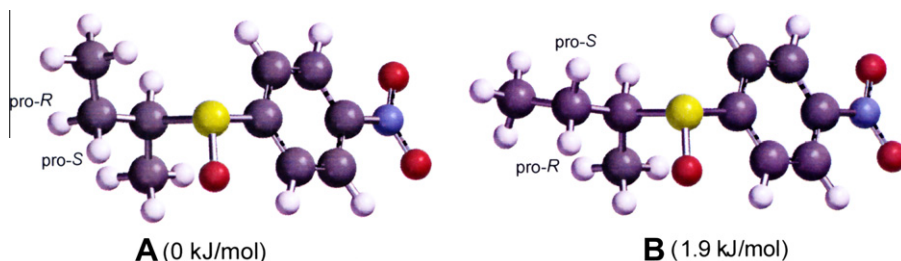


Fig. 2. Low-energy conformers **A** and **B** of (R_S, S_C)-**2d**; as calculated [15]; energy value of conformer **B** relative to that of **A**. Color code: black, carbon; white, hydrogen; red, oxygen; green-yellow, sulfur; blue, nitrogen. (For interpretation of the references to colour in this figure legend, the reader is referred to the web version of this article.)

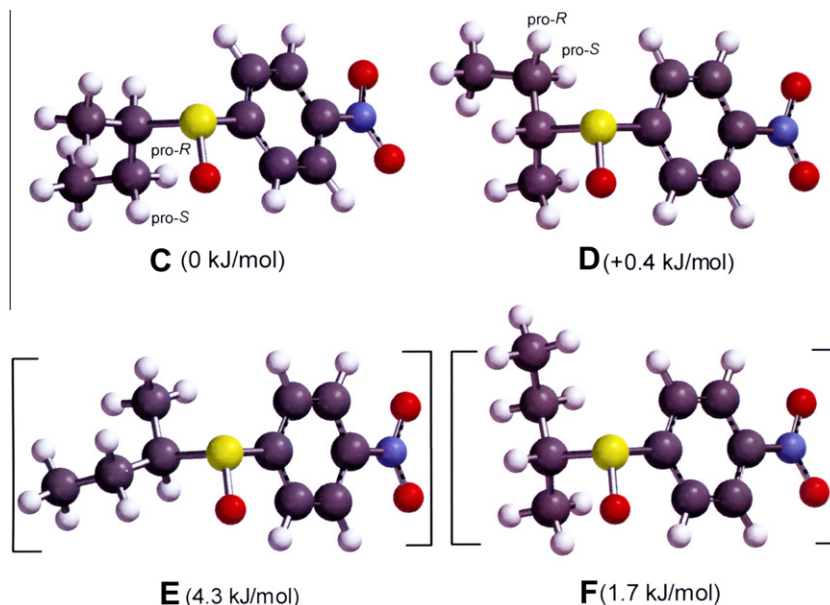


Fig. 3. Low-energy conformers **C**, **D** and **E** of (R_S, R_C) -**1d**; as calculated by MP2 methods [15]; energy values relative to that of conformer **C**. Color code: black, carbon; white, hydrogen; red, oxygen; green-yellow, sulfur; blue, nitrogen. (For interpretation of the references to colour in this figure legend, the reader is referred to the web version of this article.)

Table 4

Relative conformational energies of some conformers **A–F** of **1d** and **2d** (see Figs. 2 and 3) as calculated by density functional (B3LYP) and Møller–Plesset MP2 methods [15]; energy of **B** relative to that of **A** (*unlike*-conformers) and energies of **D–F** relative to that of **C** (*like*-conformers).

Conformational Energies (in kJ/mol)		Density functional B3LYP		Møller–Plesset MP2
		6-31G*	6-311+G**	6-31G*
1d (<i>unlike</i>)	A	0	0	0
	B	1.4	1.3	1.9
2d (<i>like</i>)	C	0	0	0
	D	1.4	1.7	0.4
	E	2.2	2.4	4.3
	F	3.6	3.8	1.7

energies: **A** (0 kJ/mol) and **B** (ca. +1.5 to +2 kJ/mol higher than **A**). Conformer **B** corresponds excellently to that obtained from the X-ray diffraction experiment (Fig. 1); conformer **A** differs from **B** basically by a rotation of the terminal ethyl group around the C–2–C–3 bond forming an *antiperiplanar* orientation of the butyl chain.

The fact that we found two conformations **A** and **B** with quite similar calculated energies (isolated molecules) is not in contrast to the existence of one sole conformer in the solid state where only **B** was observed. Stoe powder diffraction measurements were performed with both enantiomerically pure *unlike*-**2d** samples. In one case, S_S, R_C -configuration, a large number of reflections occurred so that we assume that this sample was composed of mixed crystals. On the other hand, only very few reflections were detected for the sample with R_S, S_C -configuration suggesting that only those crystals exist where the molecules adopt conformation **B** (Fig. 2). This may be explained by the recrystallization process of the two samples which may have been different with respect to external factors like solution concentrations, temperatures and, eventually, marginal impurities.

Four conformers have to be inspected in the *like*-series of diastereomers (R_S, R_C) -**1d**: **C** (0 kJ/mol), **D** (+0.4 – +1.7 kJ/mol), **E** and **F** (both ca. +2 to +4 kJ/mol) (Fig. 3, Table 3) but only **C** and **D** seem to be significant.

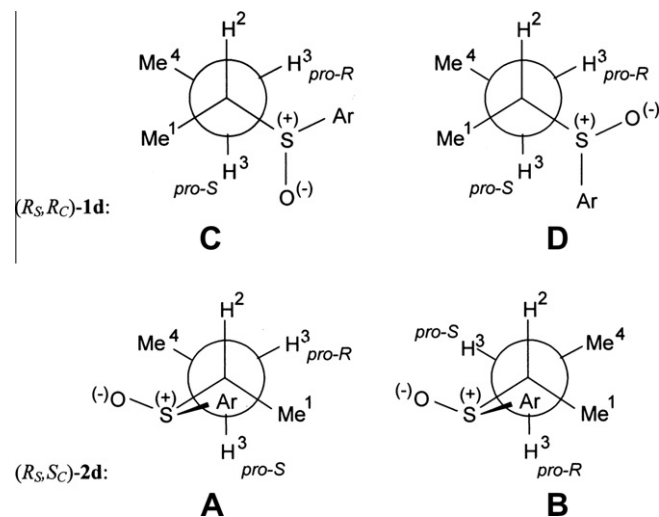


Fig. 4. Newman projections and spatial orientation of the H-2 and H-3 atoms in the conformations **C** and **D** of (R_S, R_C) -**1d** (cf. Fig. 3) as well as **A** and **B** of (R_S, S_C) -**2d** (cf. Fig. 2).

A test for the validity of the geometry calculations of the diastereomeric sulfoxides is the interpretation of the H-2/H-3 NMR signals coupled to the methyl protons H-1 and H-4. These protons form a first-order spin system in the 400 MHz ^1H NMR spectra which can be interpreted easily in terms of $^1\text{H}, ^1\text{H}$ coupling constants [19]. In each series of diastereomers the coupling constants are remarkably uniform (see footnote 'b' in Table 2) indicating that the conformational behavior is rather independent of the nature of the substituent X.

The NMR data of the relevant hydrogen atoms in (R_S, R_C) -**1d** are: $\delta(\text{H-2}) = 2.78$ ppm, $\delta(\text{H-3a}) = 1.48$ ppm and $\delta(\text{H-3b}) = 1.72$ ppm (Table 2); $^3J(\text{H-2, H-3a}) = 9.2$ Hz and $^3J(\text{H-2, H-3b}) = 4.1$ Hz indicating that the first coupling parameter is dominated by an *antiperiplanar* orientation of H-2 and H-3a whereas H-2 and H-3b are basically *gauche*-oriented [19]. By inspecting the calculated major conformers

C and **D** (Fig. 3), it turns out that the (*pro-R*)-H-3 is *gauche* to H-2 in both conformations (calculated torsion angle in **C**: $\varphi = 54.3^\circ$, in **D**: $\varphi = 65.8^\circ$); on the other hand, (*pro-S*)-H-3 is *antiperiplanar* to H-2 (calculated torsion angle in **C**: $\varphi = 170.0^\circ$, in **D**: $\varphi = -177.2^\circ$); see Fig. 4. Thus, a stereochemical assignment is possible: (*pro-R*)-H-3 is H-3b and (*pro-S*)-H-3 is H-3a. *Notabene*: this *pro-R/pro-S* assignment is opposite for the other enantiomer (S_S, S_C)-**1d**.

The situation is different for the *unlike*-isomer. For (R_S, S_C)-**2d**, the (*pro-R*)-H-3 is *gauche* with respect to H-2 in conformer **A** (calculated torsion angle $\varphi = 73.9^\circ$) but *antiperiplanar* in conformer **B** (calculated torsion angle $\varphi = -176.9^\circ$); for the (*pro-S*)-H-3 atom it is opposite (calculated torsion angle in **A**: $\varphi = -171.6^\circ$, in **B**: $\varphi = -61.2^\circ$); see Fig. 4. Consequently, the two three-bond coupling constants $^3J(\text{H-2, H-3a})$ and $^3J(\text{H-2, H-3b})$ are quite similar in their values: 7.3 and 6.6 Hz, respectively. So, a stereochemical H-3a/H-3b assignment is not possible here.

3.3. Dirhodium experiments – complexation shifts ($\Delta\delta$) and binding modes

Ligand exchange in Rh^* -adducts is fast on the NMR time-scale [5]. Therefore, NMR signals are averages of those of the complexed and the free ligands and signal shifts are defined as $\Delta\delta = \delta(\text{complexed}) - \delta(\text{free})$. Complexation shifts $\Delta\delta$ have been recorded for

Table 5
 ^1H and ^{13}C complexation shifts $\Delta\delta$ of the sulfoxides **1** and **2** after addition of an equimolar amount of Rh^* ; in ppm.^a

	1a/2a X = H (R_S, R_C)/(S_S, S_C) (R_S, S_C)/(S_S, R_C) Experiment A	1a/2a X = H (R_S, R_C)/(S_S, S_C) (R_S, S_C)/(S_S, R_C) Experiment B	1b/2b X = F (R_S, R_C)/(S_S, S_C) (R_S, S_C)/(S_S, R_C) Experiment A	1b X = F (R_S, R_C)/(S_S, S_C) (R_S, S_C)/(S_S, R_C) Experiment B	1c/2c X = Br (R_S, R_C)/(S_S, S_C) (R_S, S_C)/(S_S, R_C) Experiment A	1c/2c X = Br (R_S, R_C)/(S_S, S_C) (R_S, S_C)/(S_S, R_C) Experiment B	1d/2d X = NO ₂ (R_S, R_C)/(S_S, S_C) (R_S, S_C)/(S_S, R_C) Experiment A	1d/2d X = NO ₂ (R_S, R_C)/(S_S, S_C) (R_S, S_C)/(S_S, R_C) Experiment B	1e/2e X = OCH ₃ (R_S, R_C)/(S_S, S_C) (R_S, S_C)/(S_S, R_C) Experiment A	1e/2e X = OCH ₃ (R_S, R_C)/(S_S, S_C) (R_S, S_C)/(S_S, R_C) Experiment B
H-1	+0.20/+0.21 +0.19/+0.20	+0.20/+0.24 +0.23/+0.12	+0.25/+0.22 +0.21/+0.19	+0.12/+0.15 +0.22/+0.15	+0.21/+0.35 +0.34/+0.25	+0.23/+0.24 +0.18/+0.20	+0.22/+0.28 +0.27/+0.20	+0.18/+0.23 +0.19/+0.22	+0.26/+0.29 +0.19/+0.23	+0.20/+0.25 +0.28/+0.21
H-2	+0.65/+0.65 +0.70/+0.70	+0.57/+0.53 +0.57/+0.41	+0.75/+0.75 +0.67/+0.71	+0.25/+0.28 +0.51/+0.48	+0.69/+0.69 +0.75/+0.75	+0.74/+0.62 +0.68/+0.73	+0.78/+0.78 ^b +0.68/+0.68 ^b	+0.55/+0.58 +0.56/+0.64	+0.75/+0.75 +0.79/+0.79	+0.48/+0.32 +0.52/+0.45
H-3a ^c	+0.04/+0.07 +0.13/+0.09	+0.06/+0.11 +0.13/+0.09	+0.11/+0.10 +0.14/+0.12	+0.10/+0.09 +0.12/+0.11	+0.11/+0.14 +0.13/+0.20	+0.12/+0.13 +0.13/+0.21	+0.18/+0.18 ^b +0.18/+0.18 ^b	+0.11/+0.16 +0.11/+0.16	+0.06/+0.13 +0.16/+0.18	+0.09/+0.14 +0.08/+0.04
H-3b ^c	+0.26/+0.23 +0.34/+0.34	+0.23/+0.21 +0.22/+0.19	+0.28/+0.28 +0.30/+0.30	+0.33/+0.39 +0.31/+0.23	+0.26/+0.24 +0.33/+0.33	+0.27/+0.24 +0.30/+0.31	+0.29/+0.29 ^b +0.30/+0.30 ^b	+0.22/+0.24 +0.25/+0.30	+0.28/+0.28 +0.33/+0.33	+0.31/+0.26 +0.39/+0.23
H-4	-0.09/-0.10 -0.14/-0.09	-0.09/-0.06 -0.13/-0.06	-0.10/-0.20 -0.10/-0.12	+0.01/-0.04 -0.12/-0.07	-0.12/-0.07 -0.14/-0.09	-0.10/-0.06 -0.13/-0.11	-0.08/-0.03 -0.12/-0.08	-0.06/-0.03 -0.11/-0.09	-0.12/-0.08 -0.12/-0.09	-0.09/-0.10 -0.11/-0.13
H-2'/H-6'	+0.31/+0.28 +0.37/+0.33	+0.25/+0.17 +0.37/+0.18	+0.31/+0.46 +0.28/+0.34	+0.08/+0.17 +0.29/+0.15	+0.02/-0.07 +0.06/-0.02	+0.04/-0.06 +0.07/-0.04	+0.28/+0.21 +0.25/+0.19	+0.20/+0.16 +0.18/+0.17	+0.31/+0.22 +0.32/+0.24	+0.15/+0.23 +0.28/+0.25
H-3'/H-5'	-0.04/-0.07 -0.04/-0.08	-0.08/-0.13 -0.08/-0.07	+0.34/+0.43 +0.18/+0.24	0.00/-0.03 -0.03/+0.01	+0.08/+0.01 +0.08/-0.01	+0.11/-0.01 +0.04/-0.04	+0.19/-0.27 -0.19/-0.27	-0.19/-0.23 -0.17/-0.21	-0.10/-0.17 -0.11/-0.18/	-0.18/-0.16 -0.11/-0.12
H-4'	+0.02/+0.02 -0.03/0.00	-0.01/-0.07 -0.05/-0.09	-	-	-	-	-	-	-	-
OCH ₃	-	-	-	-	-	-	-	-	-0.04/-0.07 -0.05/-0.07	-0.08/-0.06 -0.04/-0.04
C-1	-0.6/-0.5 +0.6/+0.6	-0.5/-0.2 +0.7/+0.2	-0.5/-0.6 +0.6/+0.6	-0.5/-0.3 +0.7/+0.3	-0.5/-0.7 +0.7/+0.5	-0.5/-0.4 +0.5/+0.5	-0.5/-0.4 +0.6/+0.6	-0.4/-0.4 +0.4/+0.4	-0.6/-0.3 +0.5/+0.6	-0.5/-0.4 +0.7/+0.4
C-2	+0.8/+0.7 +0.9/+0.9	+0.7/+0.4 +0.8/+0.3	+1.0/+1.1 +1.1/+1.0	+0.4/+0.6 +0.7/+0.3	+1.0/+0.9 +0.8/+0.7	+0.9/+0.6 +0.5/+0.5	+1.0/+1.0 +0.7/+0.6	+0.7/+0.7 +0.4/+0.4	+1.0/+0.8 +0.8/+0.7	+0.6/+0.7 +0.8/+0.7
C-3	+0.3/+0.3 -1.3/-1.4	+0.1/0.0 -1.2/-0.7	+0.5/+0.0 -0.9/-0.7	+0.8/0.0 -1.1/-0.6	+0.1/-0.1 -1.2/-1.0	+0.1/+0.7 -1.2/-0.8	+0.2/+0.1 -0.9/-1.0	+0.1/+0.1 -0.9/-0.9	-0.1/-0.2 -1.1/-1.1	0.0/-0.1 -0.6/-1.1
C-4	-0.1/-0.1 -0.4/-0.4	0.0/0.0 -0.5/-0.3	-0.1/-0.1 -0.4/-0.4	+0.5/0.0 -0.4/-0.3	-0.1/-0.2 -0.5/-0.5	+0.2/+0.1 -0.5/-0.5	-0.2/-0.1 -0.6/-0.5	-0.2/-0.2 -0.5/-0.5	-0.1/-0.1 -0.5/-0.4	0.0/-0.1 -0.5/-0.5
C-1'	-2.6/-2.6 -3.0/-3.0	-2.4/-2.3 -3.3/-4.0	+0.4/+0.2 +0.1/+0.1	-2.6/-2.7 -3.0/-2.9	-3.4/-3.5 -3.6/-3.6	-3.7/-2.7 -2.8/-3.9	-3.9/-4.0 -3.1/-3.1	-2.6/-2.7 -1.8/-2.1	-2.6/-2.6 -3.3/-3.3	-4.0/-4.1 -4.6/-4.5
C-2'/C-6'	+1.0/+0.9 +1.6/+1.2	+0.9/+0.7 +1.2/+0.5	+1.2/+0.9 +1.2/+1.3	-0.1/+0.5 +1.4/+0.8	+1.0/+0.8 +1.1/+1.0	+1.0/+0.7 +0.9/+0.9	+1.0/+0.9 +1.0/+1.0	+0.8/+0.7 +0.8/+0.8	+1.1/+1.0 +1.8/+1.8	+0.3/+1.0 +1.4/+1.8
C-3'/C-5'	0.0/0.0 -0.1/0.0	-0.1/-0.1 0.0/-0.2	0.0/+0.4 0.0/-0.1	-0.2/-0.1 -0.1/-0.2	-0.1/0.0 0.0/-0.1	0.0/-0.2 -0.1/-0.6	-0.1/-0.1 -0.1/-0.1	-0.2/-0.3 -0.2/-0.3	0.0/0.0 0.0/0.0	-0.2/+0.1 0.0/-0.2
C-4'	-2.9/-2.9 -3.0/-3.0	+0.3/+0.2 +0.6/+0.1	-3.8/-3.9 -3.4/-3.1	-0.2/+0.3 +0.4/+0.1	+0.8/+0.7 +0.9/+0.8	+0.9/+0.3 +0.6/+0.8	+0.4/+0.3 -0.7/-0.8	-0.1/-0.2 -0.7/-0.7	+0.4/+0.3 +0.5/+0.4	-0.2/0.4 +0.5/0.4
OCH ₃	-	-	-	-	-	-	-	-	+0.1/-0.1 +0.1/0.0	+0.1/+0.2 +0.1/-0.1

^a Experiment A: measurement with nonracemic mixtures, Experiment B: separate measurements with pure enantiomers. Upper row in each entry are data of *like*-isomers (R_S, R_C)-**1i** and (S_S, S_R)-**1i**, lower row in each entry those of *unlike*-isomers (u) (R_S, S_C)-**2i** and (S_S, R_C)-**2i** ($i = \mathbf{a}, \mathbf{b}, \mathbf{c}, \mathbf{d}$ or \mathbf{e} , respectively); compare R/S symbols in the heading.

^b Signal overlap. No safe individual signal assignments; values are averaged.

^c Diastereotopic atoms H-3a and H-3b with $\delta(\text{H-3a}) < \delta(\text{H-3b})$ in all derivatives; for stereochemical assignments see text.

each stereoisomer in two different ways (Table 5). Enantiomers were mixed to form nonracemic mixtures so that the sets of individual NMR signals could be assigned to each enantiomer by their different signal intensities (Experiments A); this corresponds to the routine dirhodium method [5–8]. In the present study, however, we had all stereoisomers at hand so that it was of interest to perform dirhodium experiments with each of the enantiomers separately (Experiments B). Of course, we paid attention to keep external influences (concentration, molar ratios etc.) constant for all these measurements.

It turned out that differences in $\Delta\delta$ values between Experiments A and B were, indeed, found which are significant for some of the ^1H and ^{13}C nuclei; for details see Section 3.4. In general, however, the evaluation of $\Delta\delta$ values in terms of distances to binding sites is not seriously affected by the different experimental set-ups.

The largest deshieldings are observed for the H-2 and C-2 signals indicating – as expected – that the complexation site is the SO group attached to this methine. Apparently, no other hetero atom or the phenyl group can compete in the complexation, even not the methoxy oxygen atom in **1e/2e**. Neighbouring atoms may show significant signal shifts as well but these are smaller and not always consistent for all four stereoisomers of a given derivative. For example, C-1 is deshielded (+0.2 to +0.7 ppm) in all *unlike*-isomers but shielded (–0.2 to –0.5 ppm) in all *like*-isomers.

Presumably, Rh^* -phenyl group anisotropies overrule these small inductive deshieldings produced by the complexation of the latter isomers.

In previous studies on related ethers [8] and thioethers [10], we have shown that the correlation between the Hammett resonance constants σ_R^0 and the $\Delta\delta(\text{C-2}'/6')$ values is indicative of the absence (negative slope) or the presence of HOMO–LUMO orbital interaction (positive slope). The sulfoxides in the present study offer two potential binding sites, oxygen as a hard Lewis acid and sulfur as a soft Lewis acid, and it has been shown in X-ray reports that both atoms may serve as binding sites [20]. Thus, a comparison of the sulfoxide correlation with that of the ethers **3** (black diamonds in Fig. 5) and that of the thioethers **4** (magenta squares) is expected to show which of these two chalcogen atoms is favored in the adduct formation in solution.

Fig. 5 shows the dependence of C-2'/6' complexation shifts of the substituted sulfoxides on the nature of X as a function of the respective σ_R^0 values of X (green triangles for *like*- and blue ones for *unlike*-sulfoxides). In general, the complexation shifts are small, and the graphs show slightly negative slopes suggesting that the behavior of the sulfoxides is quite similar to that of the hard ether but totally different from that of the soft thioethers. Thus, the sulfoxides discussed here are hard donors barely able to form orbital (HOMO–LUMO) interactions; i.e., oxygen is the primary binding site. Fig. 6 shows the HOMO of the conformation **A** of (R_S, S_C) -**2d**; those of all other conformers and derivatives are similar. Basically, it is a π^* -orbital of the S–O bond with a contribution of aromatic π -conjugation which varies a little with the nature of X: stronger for X = NO_2 and weaker for X = F. Moreover, this orbital is sterically shielded by the adjacent phenyl and 2-butyl groups so that an approach for efficient orbital interaction with rhodium is hindered. Thus, the HOMO orbital at sulfur (Lewis base) and the LUMO of the Rh–Rh bond (Lewis acid) are “frustrated” orbitals [21].

This interpretation is corroborated by the data of *rac*-*p*-nitrophenylmethylsulfoxide (**5**; NMR data in the Experimental Part) with its slimmer methyl group, the $\Delta\delta(\text{C-2}'/6')$ value (+1.4 ppm) is significantly larger than that of the corresponding 2-butyl ana-

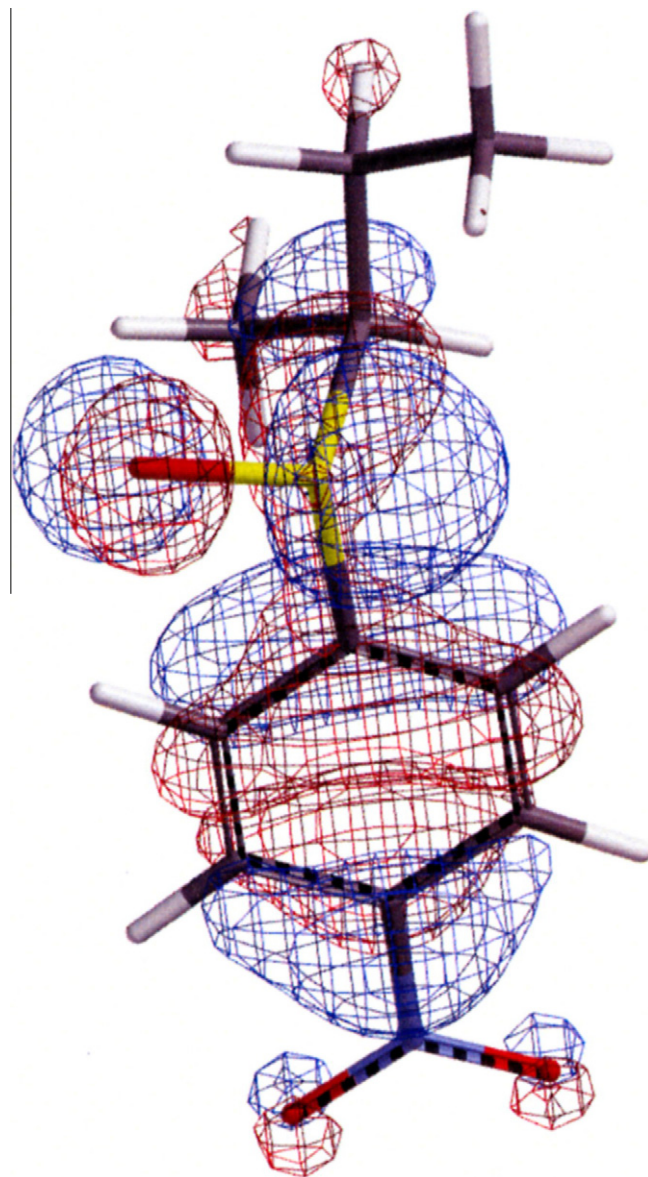
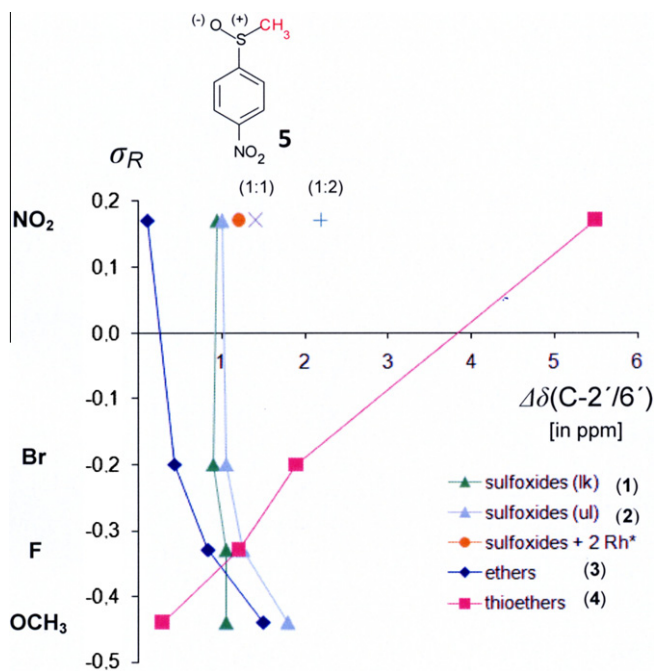


Fig. 6. HOMO of conformation **A** of (R_S, S_C) -**2d**.



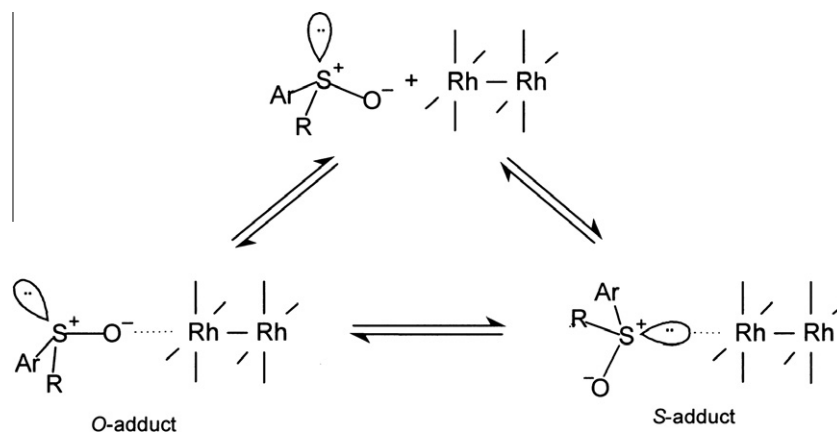


Fig. 7. Adduct formation equilibria of a sulfoxide and Rh^* .

phosphorus or sulfur, respectively, a mechanism which is associated with a reduction of the inductive effect [23].

3.4. Differentiation of enantiomers by ^1H and ^{13}C NMR signal dispersion effects ($\Delta\nu$)

Chiral ligands form diastereomeric adducts with Rh^* , and therefore, their complexations shifts are different; this difference is called diastereomeric dispersion; data are given as integers in Hz recorded at $B_0 = 9.4$ Tesla. We use the following definitions in this study:

$$\Delta\nu = \nu(R_S R_C) - \nu(S_S S_C) \quad \text{for like-sulfoxides } \mathbf{1}$$

$$\Delta\nu = \nu(R_S S_C) - \nu(S_S R_C) \quad \text{for unlike-sulfoxides } \mathbf{2}$$

Basically, dispersion effects are provoked by the anisotropy of the aromatic groups in Rh^* (ring-current effect) [24] and the difference of conformational equilibria in diastereomeric Rh^* -ligand adducts. Thereby, the averaged orientation of the Mosher residue phenyl groups is different in diastereomeric sulfoxide - Rh^* adducts exerting diverging shielding effects to nearby nuclei.

Depending on the individual atom/group orientations, the observed $\Delta\nu$ values may have positive or negative signs. As mentioned above (Section 3.3), we determined dispersion effects $\Delta\nu$ in two different ways: in nonracemic mixtures (*Experiment A*) and for single enantiomers (*Experiment B*). All these data are listed in Table 6.

The $\Delta\nu$ values of some nuclei differ considerably in the two types of experiments; even the signs of these parameters may invert when going from *Experiment A* to *B* and vice versa. Fig. 8 shows an example of enantiodifferentiation by NMR signal duplication of like-**1e**. In addition, a remarkable difference in $\Delta\nu$ is visible here: in *Experiment A* [corresponding to the spectrum section (d)] the dispersion (line distance) $\Delta\nu$ is +11 Hz whereas in *Experiment B* [corresponding to the two spectrum sections (b) and (c)] it is -7 Hz.

A similar observation is made for most of the fluorine-substituted ligand compounds where some still unidentified effects seem to reduce the complexation shifts when the ligands are enantiopure but not when they exist in mixtures [25].

The reason for these surprising differences is not entirely clear. It may originate from accidental differences in concentrations,

Table 6
 ^1H and ^{13}C diastereomeric dispersion effects ($\Delta\nu$) of the like-sulfoxides **1** [$\Delta\nu = \nu(R_S R_C) - \nu(S_S S_C)$] and the unlike-sulfoxides **2** [$\Delta\nu = \nu(R_S S_C) - \nu(S_S R_C)$] after addition of an equimolar amount of Rh^* ; in Hz at 9.4 Tesla (400.1 MHz ^1H and 100.6 MHz ^{13}C).^a

	1a/2a X = H	1a/2a X = H	1b/2b X = F	1b/2b X = F	1c/2c X = Br	1c/2c X = Br	1d/2d X = NO ₂	1d/2d X = NO ₂	1e/2e X = OCH ₃	1e/2e X = OCH ₃
	(l)/(u)	(l)/(u)	(l)/(u)	(l)/(u)	(l)/(u)	(l)/(u)	(l)/(u)	(l)/(u)	(l)/(u)	(l)/(u)
	Experiment A	Experiment B	Experiment A	Experiment B	Experiment A	Experiment B	Experiment A	Experiment B	Experiment A	Experiment B
H-1	-5/-8	-4/+44	+15/-4	-12/+28	-21/-36	-4/-8	-23/+6	-20/-12	-14/+15	-20/+28
H-2	n.d. ^b /n.d. ^b	+16/+64	n.d. ^b /n.d. ^b	-12/+12	n.d. ^b /n.d. ^b	+48/-20	n.d. ^b /n.d. ^b	-12/-32	n.d. ^b /n.d. ^b	+64/+28
H-3a ^c	-12/+14	-10/+16	n.d. ^b /n.d. ^b	+4/+4	-12/+24	-4/-32	n.d. ^b /n.d. ^b	-20/-20	n.d. ^b /+12	-20/-16
H-3b ^c	+13/n.d. ^b	+8/+22	n.d. ^b /n.d. ^b	-24/+32	+7/n.d. ^b	+12/-4	n.d. ^b /n.d. ^b	-8/-20	n.d. ^b /n.d. ^b	+20/+64
H-4	-5/+17	-12/-28	+26/+13	+20/-20	-21/+20	-16/-8	-20/+18	-12/-8	-24/+12	+4/+8
H-2'/H-6'	+18/-13	+32/+76	-44/+49	-36/+56	+36/-8	+40/+44	+27/-23	+16/+4	-34/-33	-32/+12
H-3'/H-5'	+14/-18	+20/-4	-32/-38	+12/-12	+36/-14	+48/+32	+34/-32	+24/+16	+26/-27	-8/+4
H-4'	0/0	+24/+16	-	-	-	-	-	-	-	-
OCH ₃	-	-	-	-	-	-	-	-	+11/+10	-7/+1
C-1	-37/0	-27/+46	+9/-7	-19/+43	-22/-13	-16/-3	-13/-5	-9/+1	-29/-10	-13/+34
C-2	+15/0	+26/+54	-8/+6	-21/+45	+15/-9	+30/-4	+7/-2	+5/-2	+22/-14	-13/+9
C-3	0/-11	+11/-51	+54/-31	+81/-45	+12/+20	-57/-35	+6/+8	+6/-3	+10/-3	+10/+29
C-4	0/-5	+2/-19	-9/+2	-50/-7	-5/+3	-10/+3	-7/+4	0/0	-4/+4	+4/+6
C-1'	-2/0	-4/+73	+16/-4	+10/-9	-15/n.d. ^b	-99/+107	+15/-8	-20/+1	0/0	+7/-10
C-2'/C-6'	+6/-49	+20/+63	+34/-26	-61/+61	+18/-10	+29/+2	+12/-6	+9/-4	+16/-1	-73/-13
C-3'/C-5'	0/+7	0/+14	-33/+7	-6/+13	+9/+9	+21/+49	+3/-5	+4/+4	0/0	-25/+21
C-4'	0/0	+12/+50	-8/+5	-48/+28	+12/-10	+54/-28	+9/-7	+9/0	+8/-8	-53/+7
OCH ₃	-	-	-	-	-	-	-	-	+4/-3	-23/+15

^a *Experiment A*: measurement with nonracemic mixtures, *Experiment B*: individual measurements of pure enantiomers.

^b Not detectable (n.d.) due to signal overlap; no safe individual signal assignments.

^c Diastereotopic atoms H-3a and H-3b with $\delta(\text{H-3a}) < \delta(\text{H-3b})$ in all derivatives; for stereochemical assignments see text.

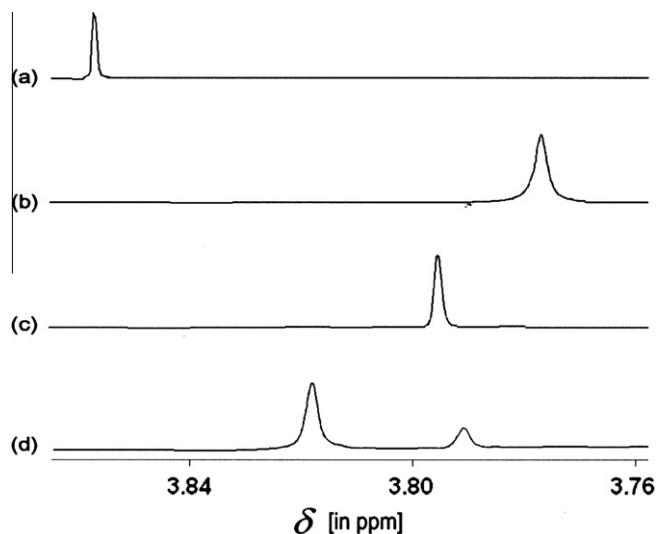


Fig. 8. Methoxy ^1H NMR signals of 4-methoxy-1-(1-methylpropylthio)benzene-S-oxide [(l)-**1e**]; (a) signal of the free ligand **1e**, (b) enantiopure (R_S,R_C)-**1e** + Rh^* (equimolar), (c) enantiopure (S_S,S_C)-**1e** + Rh^* (equimolar), and (d) nonracemic mixture of (R_S,R_C)- and (S_S,S_C)-**1e** (2.6:1) + Rh^* (equimolar).

temperatures and magnetic susceptibilities of the solutions. A more plausible source of this incongruity, however, is the stereochemistry of the adduct formation equilibria. Although a description of equilibria involving only 1:1 adducts ($\text{L} \rightarrow \text{Rh-Rh}$; cf. Fig. 7) is good enough for a semi-quantitative description of the underlying phenomena, it is over-simplified since it ignores any adducts with more than two components, as for example Rh^* bearing two ligand molecules **L**. In reality, such adducts ($\text{L} \rightarrow \text{Rh-Rh} \leftarrow \text{L}$) exist even when there is an equimolar ratio of the components Rh^* and **L** [26]. If the ligand is chiral and a mixture of both enantiomers is present – as in the case of *Experiment A* – several diastereomeric 2:1-adducts are formed due to different (+)-**L** and (–)-**L** combinations. These may differ in the averaged geometries within the Mosher acid residues from those in *Experiment B* where only one single diastereomer of 2:1-adduct exists, either two (+)-**L** or two (–)-**L** ligands [22].

In summary, however, applying the dirhodium method for enantiodifferentiation can be performed by both procedures, either using mixtures of enantiomers or by measuring both pure enantiomers separately although the magnitudes and even the signs of dispersion effects $\Delta\nu$ may vary for some ^1H and ^{13}C nuclei.

Remarkably large dispersion effects ($\Delta\nu$) can be recognized at many ^1H and ^{13}C atoms (Table 6) indicating that chiral differentiation of enantiomeric sulfoxides by NMR spectroscopy in the presence of Rh^* (dirhodium method) is easy and safe. However, in contrast to some other families of structurally related compounds studied by us earlier [23,27], the pattern of $\Delta\nu$ signs for corresponding nuclei are not consistent so that these effects – despite of their often large magnitudes – cannot be used for correlating absolute configurations of related sulfoxide derivatives. Apparently, it is the conformational flexibility of these molecules which leads to diverging atomic arrangements in the diastereomeric adducts.

4. Conclusions

- (a) Complete absolute configuration assignments of the diastereomeric *S*-chiral sulfoxides with a chiral 2-butyl residue were made by syntheses starting from enantiomerically pure thioethers, by inspecting ^1H and ^{13}C chemical shifts

and specific optical rotations $[\alpha]_D$ as well as by X-ray crystallography of some of the products. By the combination of these methods, an unequivocal differentiation between the diastereomers (*like* and *unlike*) is easily possible.

- (b) Equilibria of *O*- and *S*-adducts are formed when sulfoxides are mixed with the dirhodium complex Rh^* . If the alkyl residue *R* is bulky (2-butyl), the equilibria are shifted towards the *O*-adduct side but they move towards the *S*-adduct side if *R* is small (methyl).
- (c) The dirhodium method (enantiodifferentiation by adding Rh^*) is very effective in the case of sulfoxides whatever the adduct formation mechanism may be. It can be applied by comparing $\Delta\nu$ values of enantiomers in mix (*Experiment A*) or, alternatively, in separate NMR experiments with each of the stereoisomers (*Experiment B*). Comparing these experiments, some dispersion effects may differ considerably in magnitude and sign but this has no depriving effect on the capability of the system to discriminate the enantiomers.
- (d) The differences in the results from *Experiments A* and *B* may be explained by the admixture of 2:1-adducts in the adduct formation equilibria. In the case of *Experiment B* only one stereoisomeric 2:1 adduct exists whereas a mixture of several ones is formed in *Experiment A*.
- (e) Due to the high conformational flexibility of the sulfoxides **1** and **2** and the variation in the equilibria of adducts (*O*- vs. *S*-adducts), the dirhodium method is not safe for deriving absolute configurations of sulfoxides from the signs of their $\Delta\nu$ values.

Acknowledgements

The authors gratefully acknowledge valuable help provided by Dr. Michael Wiebcke and by Dr. S. Locmelis, Institute of Inorganic Chemistry of the Leibniz University Hannover, in the X-ray diffraction experiments and the powder diffraction measurements, respectively. This work was supported by the Deutsche Forschungsgemeinschaft (Grant Du 98/34).

References

- (a) E.B. Boyar, S.D. Robinson, *Coord. Chem. Rev.* 50 (1983) 109; (b) F.A. Cotton, R.A. Walton (Eds.), *Multiple Bonds between Metal Atoms*, second ed., Clarendon, Oxford, 1993.
- (a) C. Mertis, M. Kravaritoy, M. Chorianopoulou, S. Koinis, N. Psaroudakis, *Top. Mol. Org. Eng.* 11 (1994) 321; (b) M.P. Doyle, M.A. McKevey, T. Ye, *Modern Catalytic Methods for Organic Synthesis with Diazo Compounds: From Cyclopropanes to Ylides*, Wiley, New York, 1998; (c) A. Endres, G. Maas, *Tetrahedron* 58 (2002) 3999; (d) D.T. Nolan III, D.A. Singleton, *J. Am. Chem. Soc.* 127 (2005) 6190. and references cited therein.
- M.J. Clarke, F. Zhu, D.R. Frasca, *Chem. Rev.* 99 (1999) 2511.
- K. Wypchlo, H. Duddeck, *Tetrahedron: Asymm.* 5 (1994) 27.
- H. Duddeck, *Chem. Rec.* 5 (2005) 396. and references cited therein.
- E. Díaz Gómez, D. Albert, H. Duddeck, S.I. Kozhushkov, A. de Meijer, *Eur. J. Org. Chem.* (2006) 2278.
- H. Duddeck, E. Díaz Gómez, *Chirality* 21 (2009) 51.
- E. Díaz Gómez, H. Duddeck, *Magn. Reson. Chem.* 46 (2008) 23.
- D.V. Deubel, *Organometallics* 21 (2002) 4303.
- J.T. Mattiza, V.J. Meyer, H. Duddeck, *Magn. Reson. Chem.* 48 (2010), in press.
- J.A. Davies, F.R. Hartley, *Chem. Rev.* 81 (1981) 79. and references cited therein.
- J. Drabowicz, P. Łyżwa, M. Popielarczyk, M. Mikołajczyk, *Synthesis* 10 (1990) 937.
- C.O. Kinen, L.I. Rossi, R.H. de Rossi, *J. Org. Chem.* 74 (2009) 7132.
- See for example: (a) B. Karimi, M. Ghoreishi-Nezhad, J.H. Clark, *Org. Lett.* 7 (2005) 625; (b) M. Hirano, S. Yakabe, J.H. Clark, T. Morimoto, *J. Chem. Soc., Perkin Trans. 1* (1996) 2693; (c) A. Yamagishi, *J. Chem. Soc. Chem. Commun.* (1986) 290.
- Density functional calculations (B3LYP 6-31G*) were performed using the SPARTAN 08 program package, version 1.0.0, Wavefunction Inc., Irvine, CA; see also: Y. Shao, L.F. Molnar, Y. Jung, J. Kussmann, C. Ochsenfeld, S.T. Brown, A.T.B.

- Gilbert, L.V. Slipchenko, S.V. Levchenko, D.P. O'Neill, R.A. DiStasio Jr., R.C. Lochan, T. Wang, G.J.O. Beran, N.A. Besley, J.M. Herbert, C.Y. Lin, T. Van Voorhis, S.H. Chien, A. Sodt, R.P. Steele, V.A. Rassolov, P.E. Maslen, P.P. Korambath, R.D. Adamson, B. Austin, J. Baker, E.F.C. Byrd, H. Dachsel, R.J. Doerksen, A. Dreuw, B.D. Dunietz, A.D. Dutoi, T.R. Furlani, S.R. Gwaltney, A. Heyden, S. Hirata, C.-P. Hsu, G. Kedziora, R.Z. Khalliulin, P. Klunzinger, A.M. Lee, M.S. Lee, W.Z. Liang, I. Lotan, N. Nair, B. Peters, E.I. Proynov, P.A. Pieniazek, Y.M. Rhee, J. Ritchie, E. Rosta, C.D. Sherrill, A.C. Simmonett, J.E. Subotnik, H.L. Woodcock III, W. Zhang, A.T. Bell, A.K. Chakraborty, D.M. Chipman, F.J. Keil, A. Warshel, W.J. Hehre, H.F. Schaefer, J. Kong, A.I. Krylov, P.M.W. Gill, M. Head-Gordon, *Phys. Chem. Phys.* 8 (2006) 3172.
- [16] R.J. Abraham, J.J. Byrne, L. Griffiths, *Magn. Reson. Chem.* 46 (2008) 667.
- [17] For the nomenclature see: D. Seebach, V. Prelog, *Angew. Chem. Int. Ed. Engl.* 21 (1982) 654.
- [18] H. Duddeck, *Top. Stereochem.* 16 (1986) 219. see pp. 252f.
- [19] C.A.G. Haasnoot, F.A.A.M. de Leeuw, C. Altona, *Tetrahedron* 36 (1980) 2783.
- [20] (a) F.A. Cotton, E.V. Dikarev, M.A. Petrukhina, S.-E. Stiriba, *Inorg. Chem.* 39 (2000) 1748;
(b) C. Meyer, H. Duddeck, *Magn. Reson. Chem.* 38 (2000) 29.
- [21] See for example: J. Nyhlén, T. Privalov, *Eur. J. Inorg. Chem.* 19 (2009) 2759.
- [22] D. Magiera, J. Omelanczuk, K. Dziuba, K.M. Pietrusiewicz, H. Duddeck, *Organometallics* 22 (2003) 2464.
- [23] S. Moeller, Z. Drzazga, Z. Pakulski, K.M. Pietrusiewicz, H. Duddeck, *Chirality* 18 (2006) 395.
- [24] J.B. Lambert, E.P. Mazzola, *Nuclear Magnetic Resonance Spectroscopy – An Introduction to Principles, Applications, and Experimental Methods*, Pearson Education Inc., Upper Saddle River, NJ, 2004, pp. 62–66.
- [25] Interestingly, the fluorinated ligands form insoluble complexes with **Rh*** when the CDCl₃ solution is stored for a few hours at room temperature, occasionally even during the NMR measurements. This is not observed for any other sulfoxide.
- [26] Z. Rozwadowski, S. Malik, G. Tóth, T. Gáti, H. Duddeck, *Dalton Trans.* (2003) 375.
- [27] (a) T. Gáti, G. Tóth, J. Drabowicz, S. Moeller, E. Hofer, P.L. Polavarapu, H. Duddeck, *Chirality* 17 (2005) S40;
(b) A.G. Petrovic, P.L. Polavarapu, J. Drabowicz, Y. Zhang, O.J. McConnell, H. Duddeck, *Chem. Eur. J.* 11 (2005) 4257.